Atomistic two-temperature modelling of ion track formation in silicon dioxide

A. A. Leino[1], S. L. Daraszewicz[2], O. H. Pakarinen[1], K. Nordlund[1] and F. Djurabekova[1]

[1] *Helsinki Institute of Physics and Department of Physics, P.O. Box 43, FI-00014, University of Helsinki, Finland*
[2] *University College London, Department of Physics and Astronomy and London Centre for Nanotechnology, Gower Street, London WC1E 6BT, United Kingdom*

PACS 61.80.Jh – Ion radiation effects
PACS 61.43.Bn – Structural modeling: serial-addition models, computer simulation

Abstract – We study swift heavy ion track formation in α-quartz using the two-temperature molecular dynamics (2T-MD) model realised as a concurrent multiscale scheme. We compare the simulated track radii to the existing experimental ones obtained from small angle x-ray scattering and Rutherford backscattering experiments. The 2T-MD model provides an explanation of the origin of the track radii saturation at high electronic stopping power. Furthermore, we study the track structure and show that defects formed outside the region of density fluctuations after a swift heavy ion impact may explain the conflicting track radii produced by the two experimental techniques.

High-energy heavy ions produced by natural radioactive decay or in ion accelerators can produce micron-long and nanometer-wide damage in materials. [1–8]. These structures are called swift heavy ion (SHI) tracks (hereafter referred to as 'tracks'). They are routinely used in practical applications, such as to create holes in polymer membranes [8], in fission track dating and electronics. The explanation of the formation of the SHI tracks has been attempted through Coulomb explosion [9–11], inelastic thermal spike [3, 5, 12, 13] and exciton self-trapping models [14, 15], or combinations of these [16, 17].

The track radii measurements are often contradictory. In one of the most studied cases [3], ion tracks formed in initially high-quality quartz, two different well-established types of experiments, Rutherford backscattering-channeling (RBS-C) and small angle X-ray scattering (SAXS) give up to a factor of two difference in the track radii [18] for similar irradiation conditions.

In this Letter, we present a two-temperature molecular dynamics (2T-MD) study [7, 17], which directly links the atomistic modelling data to the SAXS and RBS-c experiments, thereby explaining the origin of the experimental discrepancy. We obtain a good quantitative agreement between the 2T-MD model and experiments and explain the origin of the track radii saturation with the electronic stopping power, S_e, defined as an average energy loss of an impinging ion per unit distance. Furthermore, by moving away from the commonly used free electron gas approximation [19] for the excited electrons, we build a more realistic two-temperature description for band-gap materials for track simulations, resulting in a fitting parameter free model.

The two-temperature model is used to describe a non-equilibrium state of matter with initially different electronic (T_e) and ionic temperatures (T_i), formed following an irradiation event. The spatiotemporal evolution of these two temperatures is assumed to be linked by the energy exchange term proportional to the effective electron-phonon (e-p) coupling strength, G [20, 21]. The model was successfully used to describe laser-matter interaction in metals [22]. Its inelastic thermal spike variant (which assumes inelastic scattering of a projectile SHI of electrons of a target material, leading to a high local T_e) was used to model SHI interaction with metals, semiconductors [23] and insulators [24, 25].

2T-MD combines a continuum model of the electronic energy transport and storage with classical MD [26] in a concurrent multiscale scheme. The electronic temperature (T_e) is assumed to evolve according to a heat diffusion equation:

$$C_e(T_e)\frac{\partial T_e}{\partial t} = \nabla \cdot (\kappa_e \nabla T_e) - G(T_e) \cdot (T_e - T_i) + A(r_\perp(v)), \quad (1)$$

where C_e is the electronic heat capacity, κ_e the elec-

tronic thermal conductivity and T_i is the local ionic temperature. The source term A describes the energy input from delta-electrons emitted perpendicularly ($r_\perp$) to SHI travelling at velocity v. Concurrently with the spatiotemporal evolution of T_e the MD is solved according to [26]:

$$m_i \frac{\partial v_i}{\partial t} = F_i(t) + \xi m_i v_i. \quad (2)$$

Here, $F_i(t)$ is the classical force on an atom i derived from the MD potential and $\xi m_i v_i$ is the additional driving term related to G. This term introduces energy exchange between the molecular dynamics equations of motion and equation 1. The magnitude of ξ is chosen to ensure energy conservation based on the 3rd term in equation 1.

The atomistic description of the two temperature model includes density changes after a phase transition, emission of shockwaves and lattice straining, defect-level description of damage and the effects of superheating on defect generation [7, 27].

We use the Munetoh parametrization of the Tersoff potential for the Si-O system [28]. We calculate the melting point (T_m) of the potential using the energy conserving coexistence method [29] and obtain (2450 ± 100) K, which is close to the experimental value (2045 K in [30]) and significantly better than other potentials (i.e. Watanabe with $T_m = 3500 \pm 500$ K [31]). The system size used was 20 nm × 20 nm × 4 nm and the simulations were run for 45 ps. During this time the temperature of the structure in the track region had decreased below the α-quartz melting point and no further track radius development was observed. Afterwards, the system was cooled to room temperature with an additional simulation. This simulation was run for 5 ps. Both ion and electron subsystems are cooled to 300 K at the borders perpendicular to ion impact direction. As in the experiments, irradiation is performed along the c-axis.

The use of a free electron gas model electronic specific heat capacity $C_e(T_e)$ leads to severely incorrect computation of T_e in excited systems even for metals [32, 33]. We obtain $C_e(T_e)$ from finite temperature generalisation [34] of density functional theory (DFT) [35, 36] using Quantum Espresso [37]. We use the local density approximation (LDA) [38], plane wave basis set of an energy cutoff 72 Ha and a 2 × 2 × 2 Monkhorst-Pack scheme k-points mesh. The electronic specific heat is evaluated from the internal energy E_e derivative with respect to the electronic temperature: $C_e(T_e) = \partial E_e / \partial T_e$. Our $C_e(T_e)$ calculation (Fig.1) accounts for the electronic density of states (DOS) [32] change and its modification at elevated T_e [39]. We note that our LDA calculations give an indirect band-gap of $E_g = 5.9$ eV (in line with the LDA result of $E_g = 5.8$ eV in [40]), which is less than the experimental value of 8.9 eV [41]. It is not straightforward to estimate the effect of this error on the final simulation results.

The electron-phonon coupling term (G) is known to strongly depend on the electronic temperature in metals

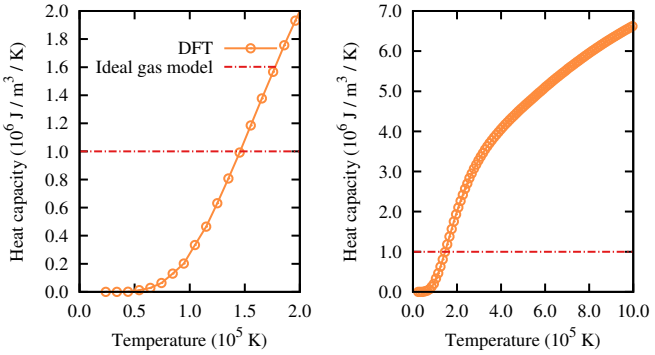

Fig. 1: On the right side, electronic temperature dependence of the specific heat capacity $C_e(T_e)$ as calculated with DFT. The dashed line shows commonly used C_e from free electron gas model assuming two excited electrons [19]. Left side shows the same data at lower temperatures for clarity.

[32] and a similar effect is expected in band-gap materials. In contrast to calculations for metals (such as the one in Ref. [42]), the standard DFT methods to obtain G for band-gap materials do not yet exist and therefore it is often fitted to yield the correct damage radius.

Moreover, the previous calculations [19] are performed so that when the temperature of the electrons becomes lower than that of the ions, the coupling between the two subsystems is turned off. Although rather arbitrary, this was considered necessary due to the following consideration. Throughout the simulation the thermal energy of the ions is too small to excite electrons to the conduction band ($k_b T << E_g$). Not much energy transfer can therefore occur from the ions to the electrons. The procedure is not needed when used a fixed relaxation time τ and a heat capacity that is calculated as a function of electronic temperature. We estimate the parameter G as a function of electronic temperature: $G(T_e) = C(T_e)/\tau$. The energy exchange between ions and electrons is then low at small temperatures (below 50 000 K) since the heat capacity is low.

The relaxation time τ can be directly obtained using a femtosecond laser together with ARPES [43] or reflectivity measurements [44]. For insulators, thus far only the decay constant of the number density of free carriers has been obtained. A value of $\tau = 150$ fs, which we use in 2T-MD, was obtained [45] for quartz, showing no significant dependence on the intensity of the laser pulse and thus T_e. This value is rather an order of magnitude estimate, which could be verified in future, more elaborate experiments.

Out of all the parameters in the 2T-MD model, the electronic diffusivity is the most poorly known. Here, we obtain it with the following rationale. The thermal spike is assumed to occur under charge neutrality, and so produces no net current of charge. Hence the Einstein–Smoluchowski relation holds, and the product of electron velocity and mean free path can be expressed as

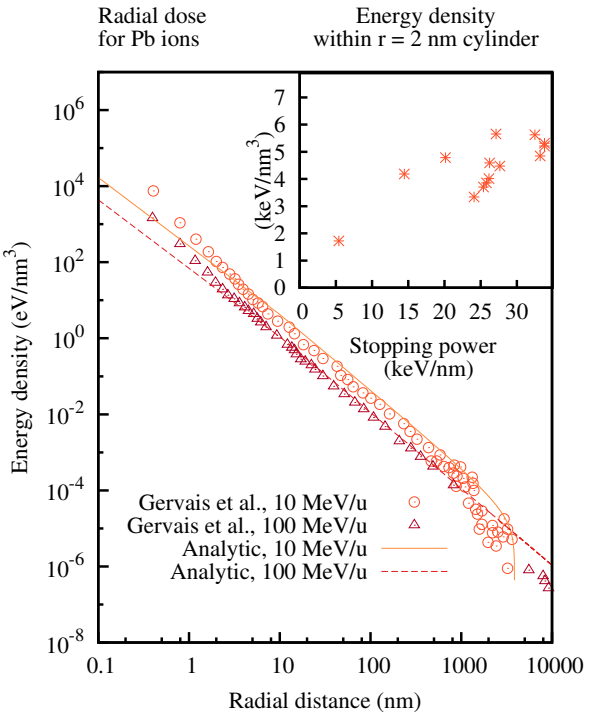

Fig. 2: A comparison between the analytical expression [49] for the delta electron distribution and the results of the Monte Carlo simulations from Ref. [47]. Inset: the energy density within r = 2 nm cylinder according to the formula given by Zhang after normalization for the ions used in Ref. [18].

$v\lambda = 3kT\mu/e$, where μ is the electron mobility. From kinetic theory, the diffusivity of heat can be expressed as $D_e = 1/3v\lambda = kT\mu/e$. The electronic mobility in silica decreases as 1/T [46]. Using the experimental values of fused quartz [46], we arrive at a constant value of $D \approx 0.6$ cm^2/s. This value provides a very good agreement with the experiments. We also tested that the agreement is not sensivitive to small (10 %) changes in the value.

The energy source term A in Eq . 1 describes the initial electronic energy distribution (assuming electron thermalization). This distribution results from the electron cascade after a SHI impact and can be calculated using Monte Carlo (MC) simulations [47] or the analytical expressions constructed from the delta-ray theory [48]. To describe A, we use the formula given by Zhang *et al.* [49], normalized to give the stopping power as predicted by SRIM [50, 51], as it gives good agreement with the MC simulations in Ref. [47]. A comparison of distributions predicted by the analytical and MC formulations in the case of Pb ions impact is given in Fig.2.

Experimentally, the track radii extracted from the SAXS data reflect the radius of the region of density contrasts due to individual tracks. Therefore, we define the track radius using the density profile calculated from the MD simulations to enable a direct comparison. However, we found that the simple step function used to fit the data from SAXS experiment [18] does not represent well the simulation data. As expected, in the simulations the density variations are not sharp. To obtain the track radius from MD data for comparison to SAXS measurements, we fit a Fermi function to the density profiles obtained from MD simulations [52] at the region of density fluctuations

$$\rho(r) = \frac{\rho_{max} - \rho_0}{\exp\left[\frac{r - r_t}{\Delta r_t}\right] + 1} + \rho_0, r > r(\rho_{max}) \qquad (3)$$

where ρ_{max} is the maximum density of the overdense shell, ρ_0 is density outside of the track and r_t is the track radius. The parameter Δr_t characterises the width of the transition from the modified density to the bulk density and therefore serves as an error estimate for the track radius. The track radii obtained from these fits reflect well the radius of the amorphized region, as seen from the circles in figure 3 and the error corresponds to the error in r from a repetitive, randomized MD simulation for a single datapoint.

The RBS-c measurements can be used to obtain the ratio of pristine channels to defected ones. With the assumption that the damage is contained in a cylindrical region, this data can be used to calculate the track radius. For qualitative comparison with RBS-c, we have identified defects by searching atoms that have broken any of their initial bonds [52]. Atoms labelled as defects are shown as the large spheres in Fig. 3.

The simulated track radii from density for the experimental SAXS ions in [18] is shown in figure 4. The figure also shows the experimental track radii for the RBS-c measurements. In contrast to the previous two temperature model or MD calculations [18], the saturation of the SAXS track radii is reproduced with good accuracy.

The reason for the saturation can be immediately seen from the inset in Fig.2. After 15 keV / nm, the energy density in the vicinity of the ions passing point does not increase linearly anymore, but saturates. The saturation is therefore a consequence of the velocity effect, which follows from the delta-ray production formulas. That is, for ions with equal stopping power, the one with a higher velocity will deposit its energy in a broader area. This reflects the fact that increasing the ion velocity will also increase the electron velocity in a collision and lead to a longer electron range.

While not both RBS-c datasets indicate saturation, it can be seen that the RBS-c radii are systematically higher than the SAXS radii at high stopping powers. To analyze the cause of this difference, we have plotted the radius at which the defect concentration falls below 1% as measured from the center of the track in figure 4. This threshold was chosen based on a reasonable error limit in a RBS-c experiment [54] in defect sensitivity for a qualitative comparison. It can be seen that at high stopping powers, the defected track extends to a notably larger region than the one with density fluctuations. We find these observations as compelling evidence to explain the discrepancies between the

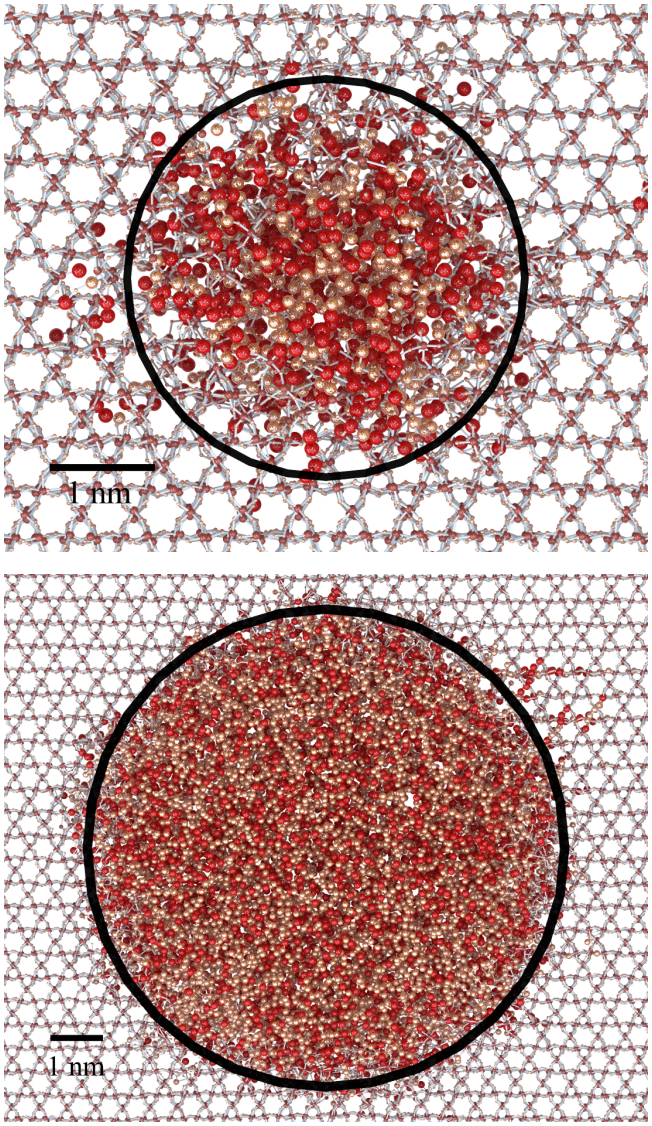

Fig. 3: Snapshot of a relatively small track (27 MeV Au, top) and a bigger one at the saturation region (1.4 GeV Au, bottom). The circles are the track radii that are obtained by fitting the parameters in equation 3 and atoms labelled as defects are drawn as large spheres.

two techniques. It should be also noted that these features cannot be included in a continuum description of the heat spike model.

In conclusion, we have studied track formation in silicon dioxide using two-temperature molecular dynamics. We have shown that within this model, the SAXS measurements of the track radius can be faithfully reproduced. Moreover, our simulations indicate that the differences in SHI track radii yielded between the RBS-c and SAXS techniques could be consequence of their sensitivity to different kind of defective structures.

Taken together, these results indicate a heat spike model describes well track formation in SiO_2. The inelastic thermal spike model can be readily applied to other insulating materials, provided that an accurate electronic heat capacity is given, and implemented with an atomistic description of the lattice melting and defect formation.

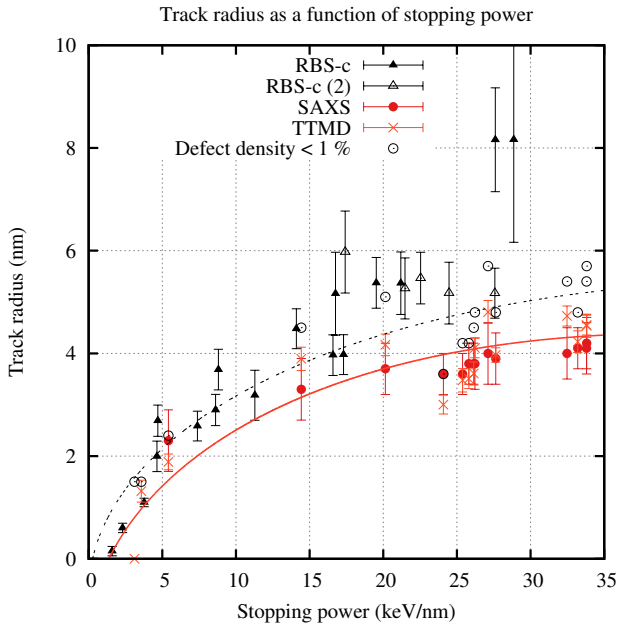

Fig. 4: Track radius as a function of stopping power. The experimental data are from Refs. [3, 18, 53]. Note that the simulated ions are the SAXS ions in Ref. [18] and that in the calculations surface stopping powers are used for simplicity. Therefore the SAXS track radii errorbars are constructed from track polydispersity (change in track radius along the track) and its error. The lines are polynomial fits to the simulation data points to guide the eye. The empty circles indicate a radius at which the defect concentration falls below 1% in the simulations.

* * *

Acknowledgements. – SD is funded by EPSRC under the M3S IDTC and CCFE. AL thanks Boshra Afra for useful discussions and NGS-nano and the Academy of Finland for funding.

REFERENCES

[1] Fleischer R. L., Price P. B. and Walker R. M., *J. Appl. Phys.*, **36** (1965) 3645.
[2] Gallagher K., Brown R. and Johnson C., *Annu. Rev. Earth. Pl. Sc.26*, **1998** (519) .
[3] Meftah A., Brisard F., Costantini J. M., Doorhee E., Hage-Ali M., Hervieu M., Stoquert J. P., Studer F. and Toulemonde M., *Phys. Rev. B*, **49** (1994) 12457 .
[4] Kanjijal D., *Curr. Sci.*, **80** (2001) 1560.
[5] Toulemonde M., Assmann W., Dufour C., Meftah A., Studer F. and Trautmann C., *Mat. Fys. Medd. Kong. Dan. Vid. Selsk.*, **52** (2006) 263.

[6] Lang M., Lian J., Zhang F., Hendriks B. W., Trautmann C., Neumann R. and Ewing R. C., *Earth Planet. Sc. Lett.*, **274** (2008) 355.

[7] Kluth P., Schnohr C. S., Pakarinen O. H., Djurabekova F., Sprouster D. J., Giulian R., Ridgway M. C., Byrne A. P., Trautmann C., Cookson D. J., Nordlund K. and Toulemonde M., *Phys. Rev. Lett.*, **101** (2008) 175503.

[8] Weber W. J., Duffy D. M., Thom L. and Zhang Y., *Current Opinion in Solid State and Materials Science*, **19** (2015) 1 .

[9] Klaumünzer S., Hou M. D. and Schumacher G., *Phys. Rev. Lett.*, **57** (1986) 850.

[10] Bringa E. M., *Nucl. Instr. Meth. Phys. Res. B*, **209** (2003) 1.

[11] Cherednikov Y., Sun S. N. and Urbassek H. M., *Phys. Rev. B*, **87** (2013) 245424.

[12] Trautmann C., Klaumünzer S. and Trinkaus H., *Phys. Rev. Lett.*, **85** (2000) 3648.

[13] Wang Z. G., Dufour C., Paumier E. and Toulemonde M., *J. Phys.: Condens. Matt.*, **6** (1994) 6733.

[14] Itoh N., *Nucl. Instr. Meth. Phys. Res. B*, **116** (1996) 33 .

[15] Itoh N., Duffy D. M., Khakshouri S. and Stoneham A. M., *J. Phys.: Condens. Matter*, **21** (2009) 474205.

[16] Bringa E. M. and Johnson R. E., *Phys. Rev. Lett.*, **88** (2002) 165501.

[17] Ridgway M., Bierschenk T., Giulian R., Afra B., Rodriguez M. D., Araujo L., Byrne A. P., Kirby N., Pakarinen O. H., Djurabekova F., Nordlund K., Schleberger M., Osmani O., Medvedev N., Rethfeld B., Wesch W. and Kluth P., *Phys. Rev. Lett.*, **110** (2013) 245502.

[18] Afra B., Rodriguez M. D., Trautmann C., Pakarinen O. H., Djurabekova F., Nordlund K., Bierschenk T., Giulian R., Ridgway M. C., Rizza G., Kirby N., Toulemonde M. and Kluth P., *J. Phys.: Condens. Matter*, **25** (2013) 045006.

[19] Toulemonde M., Dufour C., Meftah A. and Paumier E., *Nucl. Instr. Meth. Phys. Res. B*, **166 - 167** (2000) 903 .

[20] Seitz F. and Köhler J., *Sol. St. Phys.*, **2** (1956) 305.

[21] Kaganov M., Lifshitz I. and Tanatarov L., *JETP*, **173** (1956) .

[22] Fujimoto J. G., Liu J. M., Ippen E. P. and Bloembergen N., *Phys. Rev. Lett.*, **53** (1984) 1837.

[23] Chettah A., Kucal H., Wang Z., Kac M., Meftah A. and Toulemonde M., *Nucl. Instr. Meth. Phys. Res. B*, **267** (2009) 2719.

[24] Meftah A., Costantini J., Khalfaoui N., Boudjadar S., Stoquert J., Studer F. and Toulemonde M., *Nucl. Instr. Meth. Phys. Res. B*, **237** (2005) 563.

[25] Toulemonde M., Assmann W., Dufour C., Meftah A., Studer F. and Trautmann C., *Mat. Fys. Medd.*, **52** (2006) 263.

[26] Ivanov D. and Zhigilei L., *Phys. Rev. B*, **68** (2003) .

[27] Duffy D. M., Itoh N., Rutherford A. M. and Stoneham A. M., *J. Phys.: Condens. Matter*, **20** (2008) 082201.

[28] Munetoh S., Motooka T., Moriguchi K. and Shintani A., *Comp. Mater. Sci.*, **39** (2007) 334 .

[29] Morris J. R., Wang C. Z., Ho K. M. and Chan C. T., *Phys. Rev. B*, **49** (1994) 3109.

[30] Haynes W., *CRC Handbook of Chemistry and Physics, 95th Edition* (Taylor & Francis) 2014.

[31] Leino A. A., Pakarinen O. H., Djurabekova F., Nordlund K., Kluth P. and Ridgway M. C., *Mater. Res. Lett.*, **2** (2014) 37.

[32] Lin Z., Zhigilei L. and Celli V., *Phys. Rev. B*, **77** (2008) 075133.

[33] Giret Y., Gellé A. and Arnaud B., *Phys. Rev. Lett.*, **106** (2011) 155503.

[34] Mermin N., *Phys. Rev.*, **137** (1965) A1441.

[35] Hohenberg P., *Phys. Rev.*, **136** (1964) B864.

[36] Kohn W. and Sham L. J., *Phys. Rev.*, **140** (1965) A1133.

[37] Giannozzi P., Baroni S., Bonini N., Calandra M., Car R., Cavazzoni C., Ceresoli D., Chiarotti G. L., Cococcioni M., Dabo I., Dal Corso A., de Gironcoli S., Fabris S., Fratesi G., Gebauer R., Gerstmann U., Gougoussis C., Kokalj A., Lazzeri M., Martin-Samos L., Marzari N., Mauri F., Mazzarello R., Paolini S., Pasquarello A., Paulatto L., Sbraccia C., Scandolo S., Sclauzero G., Seitsonen A. P., Smogunov A., Umari P. and Wentzcovitch R. M., *J. Phys.: Condens. Matter*, **21** (2009) 395502 (19pp).

[38] Ceperley D. M., *Phys. Rev. Lett.*, **45** (1980) 566.

[39] Mazevet S., Clrouin J., Recoules V., Anglade P. and Zerah G., *Phys. Rev. Lett.*, **95** (2005) 085002.

[40] Sevik C. and Bulutay C., *J. Mater. Sci.*, **42** (2007) 6555.

[41] Laughlin R. B., *Phys. Rev. B*, **22** (1980) 3021.

[42] Arnaud B. and Giret Y., *Phys. Rev. Lett.*, **110** (2013) 016405.

[43] Johannsen J. C., Ulstrup S., Cilento F., Crepaldi A., Zacchigna M., Cacho C., Turcu I. C. E., Springate E., Fromm F., Raidel C., Seyller T., Parmigiani F., Grioni M. and Hofmann P., *Phys. Rev. Lett.*, **111** (2013) 027403.

[44] Brorson S. D., Kazeroonian A., Moodera J. S., Face D. W., Cheng T. K., Ippen E. P., Dresselhaus M. S. and Dresselhaus G., *Phys. Rev. Lett.*, **64** (1990) 2172.

[45] Audebert P., Daguzan P., Dos Santos A., Gauthier J. C., Geindre J. P., Guizard S., Hamoniaux G., Krastev K., Martin P., Petite G. and Antonetti A., *Phys. Rev. Lett.*, **73** (1994) 1990.

[46] Hughes R. C., *Phys. Rev. Lett.*, **30** (1973) 1333.

[47] Gervais B. and Bouffard S., *Nucl. Instr. Meth. Phys. Res. B*, **88** (1994) 355 .

[48] Kobetich E. J. and Katz R., *Phys. Rev.*, **170** (1968) 391.

[49] Zhang C., Dunn D. E. and Katz R., *Phys. Rev.*, **170** (1968) 391.

[50] Ziegler J. F., SRIM-2008.04 software package, available online at *http://www.srim.org*. (2008).

[51] Toulemonde M., Costantini J., Dufour C., Meftah A., Paumier E. and Studer F., *Nucl. Instr. Meth. Phys. Res. B*, **116** (1996) 37 .

[52] Leino A. A., Daraszewicz S. L., Pakarinen O. H., Djurabekova F., Nordlund K., Afra B. and Kluth P., *Nucl. Instr. Meth. Phys. Res. B*, **326** (2013) 289.

[53] Tombrello T., *Nucl. Instr. Meth. Phys. Res. B*, **2** (1984) 555 .

[54] Bianconi M., Albertazzi E., Balboni S., Colombo L., Lulli G. and Satta A., *Nucl. Instr. Meth. Phys. Res. B*, **230** (2005) 185 .